Colloids and Interface Science Communications 5 (2015) 8–11

Contents lists available at ScienceDirect

Colloids and Interface Science Communications

journal homepage: www.elsevier.com/locate/colcom

Rapid Communication

Adsorption of water vapor on mesoporosity-controlled singe wall carbon nanohorn

Elda Zoraida Pina-Salazar, Katsumi Kaneko *

Center for Energy and Environmental Science, Shinshu University, 4-17-1 Wakasato, Nagano 380-8553, Japan

ARTICLE INFO

Article history:
Received 13 April 2015
Accepted 18 May 2015
Available online 29 May 2015

Keywords:
Water adsorption
Hydrophobic mesopores
Single wall carbon nanohorn
Nanowindow
Water cluster

ABSTRACT

The adsorption mechanism of water vapor in hydrophobic carbon mesopores is not clearly understood. Single wall carbon nanohorns (SWCNH) having different tube diameters in the range of 2 to 6 nm were oxidized at a lower temperature than the widely used temperature of 823 K. Oxidation at 633 K can selectively open thinner tubes of SWCNH and then the oxidation at different times can control the mesoporosity. The porosity of thus-oxidized SWCNH was evaluated from the nitrogen adsorption isotherms at 77 K. The pore volume ratio of micropores to mesopores was in the range of 0.50 to 0.90. The linear relationship between water adsorption amount and the pore volume of micropores and small mesopores (<5 nm) was observed, showing that water molecules are adsorbed even in small mesopores by the cluster-mediated filling mechanism as well as in micropores.

Carbon surfaces are basically hydrophobic, although the contact angle of graphite surfaces for liquid water is still controversial [1,2]. Water vapor is not adsorbed on crystalline carbon blacks below $P/P_0 = 0.9$ [3]. On the other hand, water molecules are adsorbed on activated carbon without oxidation treatment even below $P/P_0 = 0.9$ [4,5]. For example, the adsorption isotherm of pitch-based activated carbon fibers (ACFs) on which surface functional groups are the least of various ACFs rises steeply above $P/P_0 = 0.5$, depending on the pore width; the larger the pore width, the larger the rising P/P_0 [6]. Furthermore, the adsorption amount is often larger than 1 g-water per g-carbon. This rising pressure is not described by the Kelvin equation and therefore the adsorption of water vapor on activated carbons is not described by the conventional capillary condensation mechanism [7]. Ohba et al. have shown that cluster formation of water molecules is indispensable to induce the predominant water adsorption on activated carbon above $P/P_0 = 0.5$; they indicated that the size of the water clusters should match with pore width [8]. Hanzawa and Kaneko explicitly showed that water molecules were not adsorbed in mesopores of 28 nm in width, but in micropores of 0.7 nm in width in case of activated carbon aerogel [7]. However, still we do not understand adsorption of water in small carbon mesopores whose width is less than 10 nm, although Thommes et al. started to study water vapor adsorption on ordered mesoporous carbon [9].

Single Wall Carbon Nanohorn (SWCNH) are one of the single wall carbon nanotubulites, being better characterized porous carbons than activated carbon [10]. Transmission electron microscopic (TEM) observations showed that a SWCNH particle had a tube and a tip structure, where the tube diameter was in the range of 2 to 6 nm [10]. Raman spectroscopy and electrical conductivity studies elucidated that the single carbon wall of SWCNH was less-crystalline, being different from single wall carbon nanotube. Utsumi et al. reported that simple oxidation using oxygen gives nanoscale windows on the single graphene wall; the oxidation at 823 K provides the high surface area of 1420 $m^2\ g^{-1}$ due to formation of nanoscale windows (nanowindows) on the graphene wall [10]. Consequently, SWCNH having nanowindows, are an optimum model of porous carbons for the study on the relationship between water adsorption and small mesoporosity, whose width is less than 6 nm. This article reports water vapor adsorption isotherms of SWCNH of different mesoporosity obtained by oxidation at temperatures lower than 823 K.

SWCNH was purchased from NEC (purity >85%), and it was used without further purification. The main impurity is graphite. Thermal gravimetric (TG) analysis of SWCNH was carried out under flow of a He (80%)-O_2 (20%) mixed gas with a flow rate of 10 K min^{-1}. Evolved gases during the TG measurement were analyzed by mass spectrometry (TG-DTA-PIMS, Rigaku Co.). We oxidized SWCNHs at temperatures lower than 823 K which gave the highest porosity in the preceding study SWCNHs were oxidized in the temperature range of 573 to 633 K under the He-O_2 mixed gas (100 mL min^{-1}) for different periods of "zero" to 12 h. Here "zero" means that oxidation stopped just after reaching the target temperature. Since oxidation at 823 K should produce nanoscale windows whose size is widely distributed, oxidation temperatures as low as 633 K in reference to TG results were used (Fig. S1).

The nanoporosity of SWCNH samples oxidized at different conditions was determined by N_2 adsorption at 77 K using a volumetric apparatus (Quantachrome-Autosorb IQ2). The N_2 adsorption isotherms

* Corresponding author.
E-mail address: kkaneko@shinshu-u.ac.jp (K. Kaneko).

http://dx.doi.org/10.1016/j.colcom.2015.05.002

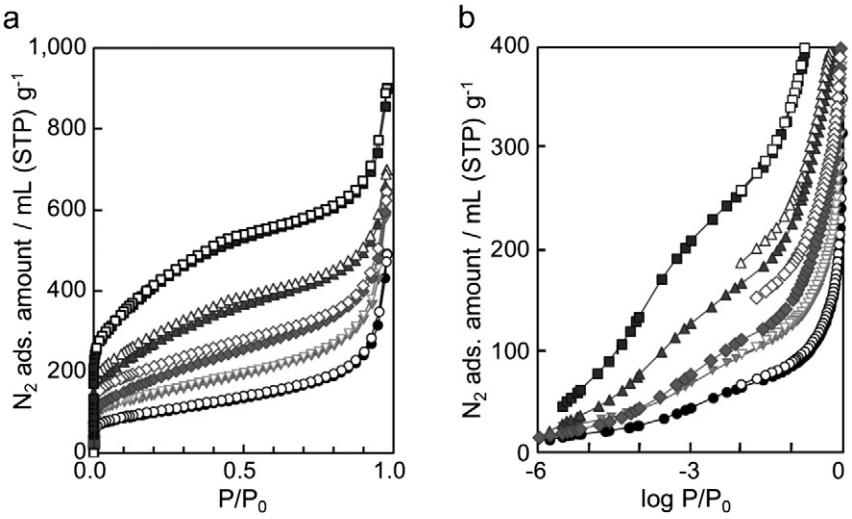

Fig. 1. N_2 adsorption isotherms of SWCNH samples at 77 K. Pristine SWCNH (●), SWCNH oxidized at 573 K for 2 h (▼), 633 K for 0 h (♦); for 4 h (▲) and for 12 h (■). a) P/P_0 is expressed in the linear scale and b) logarithmic scale. Close and open symbols indicate adsorption and desorption branches, respectively.

were analyzed by the Subtracting Pore Effect (SPE) method using the α_s plot [9] and the Quenched Solid Density Functional Theory (QS-DFT) [10] to provide the pore structural parameters and pore size distributions. Infrared spectra of the SWCNH before and after oxidation treatment in the range of 1000 to 4000 cm^{-1} were obtained with the KBr method on an FT-IR spectrometer (Nicole 6700 FT-IR). Temperature-programed desorption (TPD) profiles of the SWCNH before and after the oxidation treatment were measured in the temperature range of 373 to 1273 K under He flow of 300 mL min^{-1} at a heating rate of 10 K min^{-1} using the apparatus TG-DTA-PIMS (Rigaku Co.). Prior to this measurement, samples were degased for 2 h under vacuum at 393 K. The water vapor adsorption isotherms of SWCNH were measured at 298 K with a volumetric equipment using Quantachrome-Hydrosorb after pretreating at 423 K and 2 mPa for 2 h.

Fig. 1a shows N_2 adsorption isotherms of SWCNH oxidized at different conditions. The N_2 adsorption isotherm of closed SWCNH (before oxidation) is of typical IUPAC Type II, indicating minor contribution of micropores and mesopores. Oxidation of SWCNH at 633 K varies the shape of the adsorption isotherm and increases remarkably the adsorption amount. These adsorption isotherms have the nature of Type I and Type II, indicating the marked increase of microporosity and mesoporosity coming from small mesopores. Consequently, nanowindows are produced in the graphene walls of SWCNH by the oxidation treatments [11]. Also, a slight low pressure adsorption hysteresis is observed; the narrow hysteresis loop does not close up to the vertical axis, in particular, for oxidized SWCNH samples except for SWCNH oxidized at 633 K for 12 h. This hysteresis should come from the restricted diffusion of the N_2 molecules at the nanowindows, suggesting that the size of the nanowindows is smaller than the bi-molecular size of the N2 molecule (0.7 nm) [12]. The oxidation at 633 K for 12 h, increases the nanowindows size. The adsorption behavior in the P/P_0 range of 10^{-6} to 10^{-3} (Fig. 1b) suggests an intensive growth of micropores by the oxidation for a longer time.

Fig. 2a shows the high resolution α_s plots of the N_2 adsorption isotherms. The high resolution α_s plots have an upward deviation of filling swing below $\alpha_s = 0.5$. The filling swing as well as the condensation swing ($>\alpha_s = 0.5$) of SWCNH oxidized at 633 K for 12 h is the most predominant. Analyzing these α_s plots provides the average pore parameters of SWCNH samples, as shown in Table 1.

Almost all oxidations other than oxidation at 573 K for 2 h increase significantly the surface area and the micropore volume. In particular, oxidation at 633 K for 12 h gives the largest surface area and pore volume, being close to the published results (1420 $m^2\ g^{-1}$) of SWCNH oxidized at 823 K. The N_2 adsorption isotherms were analyzed by the QS-DFT method using the cylindrical pore model to obtain the pore size distributions, as shown in Fig. 2b. Non-oxidized SWCNH has micropores with slight mesopores whose width is smaller than 5 nm. The pore volume ratio of micropores to mesopores was determined from the pore size distribution, as listed in Table 1. The open SWCNH obtained by milder oxidation has a larger pore volume of micropores to mesopores, indicating that the milder oxidation produces nanowindows in SWCNHs of

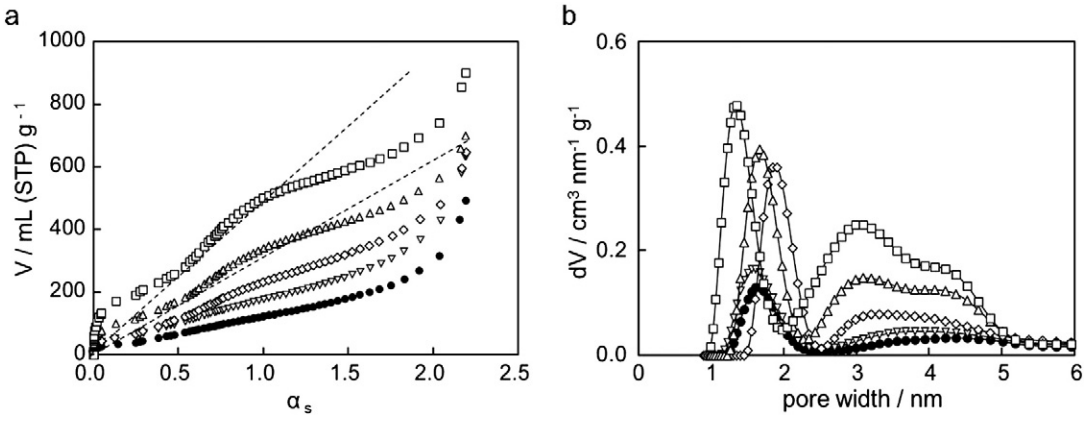

Fig. 2. a) α_s plots of the N_2 adsorption isotherms at 77 K and b) pore size distributions of SWCNH samples by QS-DFT for cylindrical pores. Pristine SWCNH (●) and SWCNH oxidized at 573 K for 2 h (▽), 633 K for 0 h (◇), 4 h (△) and 12 h (□).

Table 1
Pore parameters of pristine SWCNH and SWCNH oxidized at different conditions from N_2 adsorption isotherms.

Oxidation conditions	Surface area[a]	Micropore volume (QS-DFT)	Micropore volume (DR[b])	Total pore volume at $P/P_0 = 1$	Micro/mesopore volume ratio[c]
	$[m^2\ g^{-1}]$	$[cm^3\ g^{-1}]$	$[cm^3\ g^{-1}]$	$[cm^3\ g^{-1}]$	
Pristine	445	0.065	0.170	0.94	0.90
573 K for 2 h	490	0.092	0.200	1.17	0.90
633 K for 0 h	600	0.120	0.240	1.16	0.60
633 K for 4 h	870	0.190	0.330	1.20	0.60
633 K for 12 h	1380	0.240	0.480	1.52	0.50

[a] The surface area is determined by subtracting pore effect (SPE) method.
[b] This value is determined from Dubinin–Radushkevich (DR) plot for the P/P_0 range of 1.0×10^{-4} to 1.0×10^{-2}.
[c] The ratio of micropore volume against mesopore volume of mesopores smaller than 5 nm, which is determined from the pore size distribution with QS-DFT method.

smaller diameter. It is well known that oxidation begins at the pentagons in the cap of carbon nanotube families [13,14]. Hence, oxidation starts at the pentagons in the tip of SWCNH whose tube diameter is smaller. The microporosity/mesoporosity ratio is in the range of 0.50 to 0.90. These SWCNH samples are appropriate for the study on the effect of small mesopores on observable water adsorption.

As water adsorption is sensitively affected by surface functional groups due to its ability to form hydrogen bonds [5], the surface functional groups were determined by FT-IR spectroscopy, as shown in Fig. S2. Characteristic vibration modes at 1100, 1380, 1600, 2920 and 3400 cm^{-1}, were assigned to the stretching vibration modes of C–O groups, C–OH groups, C=C of benzene ring, C–H of methylene group and O–H group, respectively [15,16]. The oxidation of SWCNH at 633 K for 12 h increases the peak intensities of the C–OH and the C–O. On the contrary, the peak intensity of the C=C mode does not change significantly.

We can refer to the established assignment of the evolved CO and CO_2 to different kinds of surface functional groups [17–19]. The observed TPD profile of SWCNH oxidized at 633 K for 12 h shows two stronger evolution peaks of CO_2 centered at 649 K and 760 K than the non-oxidized SWCNH, as shown in Fig. S3. Specifically, the area under the curve of the evolution of CO_2 from 573 to 698 K (highest signal at 649 K), and from 698 to 823 K (highest signal at 760 K) are larger by about 2 times for the oxidized SWCNH than the non-oxidized SWCNH (Fig. S3). Evolution of CO_2 from the samples must indicate the presence of carboxyl, carboxyl anhydrous and lactone groups on the SWCNH structure, which decompose as CO_2 [19]. It is worth pointing out that the density of surface functional groups of the oxidized SWCNH is nearly half of that of the pristine SWCNH. Therefore, these functionalities should be located mainly as active sites on the edges of the nanowindows created by the oxidation, as Bekyarova et al. suggested [18]. Fig. 3a shows water adsorption isotherms of SWCNH samples at 298 K. Adsorption below $P/P_0 = 0.3$ for all SWCNH samples is negligibly small, indicating that these samples are hydrophobic, even though the surface functional groups, are detected by the FT-IR and TPD examinations (Figs. S2 and S3, respectively). The predominant water adsorption starts above $P/P_0 = 0.6$ for all samples, accompanying with an explicit adsorption hysteresis. The water adsorption isotherms are similar to those of hydrophobic ACFs which have only micropores whose width is smaller than 1.5 nm. The rising P/P_0 of the adsorption branch of the adsorption isotherm of ACFs depends on the pore width; the larger the pore width, the larger the rising P/P_0 [6]. The hysteresis loop of water adsorption isotherms of ACFs also depends on the pore width [20]. On the other hand, the basic frame of the adsorption hysteresis loop of the SWCNH samples is almost similar to each other, as shown in Fig. 3b, suggesting that water molecules are adsorbed with similar mechanism. However, the rising P/P_0 value of SWCNH oxidized is slightly larger than that of the pristine SWCNH. In particular, the rising P/P_0 of the SWCNH oxidized at 633 K for 12 h is the smallest among the samples regardless of only small difference. This should be associated with a slight adsorption below $P/P_0 = 0.4$. The inset in Fig. 3b shows the adsorption branches of the normalized water adsorption isotherms below $P/P_0 = 0.3$. The larger slope of the adsorption isotherm in this range indicates the presence of more surface functional groups [4] (Fig. S4). Correspondingly the SWCNH sample oxidized at 633 K for a longer period of time has the largest slope. Hence the presence of more surface functional groups promotes the cluster filling of water molecules at a smaller rising P/P_0. Nevertheless, this promotion of the cluster filling by the surface functional groups is too limited to influence the adsorption mechanism.

The cluster-mediated filling mechanism is applied to water adsorption on typical microporous carbons. We need to examine the applicability of cluster-mediated filling mechanism to adsorption of water on

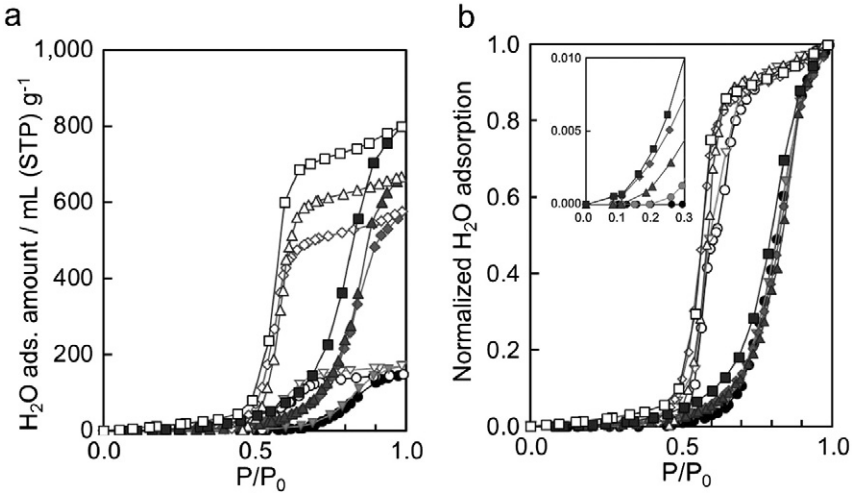

Fig. 3. Water adsorption isotherms of SWCNH samples at 298 K; pristine (●) and oxidized at 573 K for 2 h (▼), 633 K for 0 h (♦); 4 h (▲) and 12 h (■). Here the water adsorption amount of Fig. 3b is normalized using the saturated adsorption amount. Close and open symbols indicate adsorption and desorption branches, respectively.

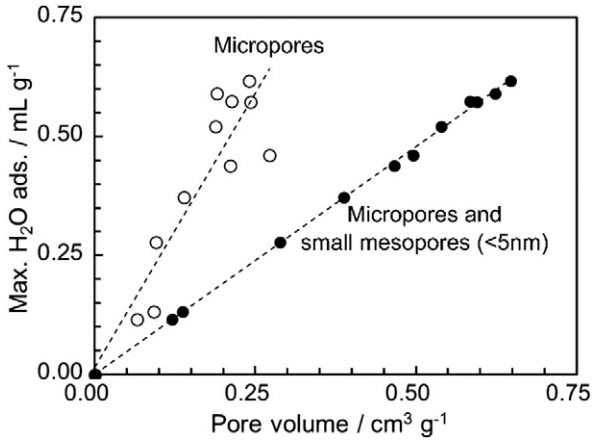

Fig. 4. Relation between water adsorbed and pore volume of the SWCNH samples.

carbon mesopores using SWCNH samples having different mesoporosity. We find a linear correlation between the maximum amount of water adsorbed and the total pore volume of micropores and mesopores not larger than 5 nm, as shown in Fig. 4. The linear relation supports that water adsorption even in small mesopores occur in the same way as in micropores. Water molecules are not adsorbed in micropores by capillary condensation [7], but by cluster-mediated filling mechanism. We must study the adsorption process using small angle X-ray scattering in order to obtain the information on the structure change of adsorbed water in small carbon mesopores with P/P_0 in future.

The authors are thankful to the Grant-in-Aid for Scientific Research (A) (24,241,038) and partially support by the Center of innovation Program from Japan Science and Technology Agency, JST.

Appendix A Supplementary data

Supplementary data to this article can be found online at http://dx.doi.org/10.1016/j.colcom.2015.05.002.

References

[1] F.M. Fowkes, W.D. Harkins, The state of monolayers adsorbed at the interface solid-aqueous solution, J. Am. Chem. Soc. 62 (1940) 3377–3386.
[2] M.E. Shrader, Ultrahigh-vacuum techniques in the measurement of contact angles. LEED study of the effect of structure on the wettability of graphite, J. Phys. Chem. 84 (1980) 2774–2779.
[3] M. Asai, T. Ohba, T. Iwanaga, H. Kanoh, M. Endo, J. Campos-Delgado, M. Terrones, K. Nakai, K. Kaneko, Marked adsorption irreversibility of graphitic nanoribbons for CO_2 and H_2O, J. Am. Chem. Soc. 133 (2011) 14,880–14,883.
[4] I.I. Salame, T.J. Bandosz, Experimental study of water adsorption on activated carbons, Langmuir 15 (1999) 587–593.
[5] K. Kaneko, Water capture in carbon cuboids, Nat. Chem. 7 (2015) 194–196.
[6] J. Miyawaki, T. Kanda, K. Kaneko, Hysteresis-associated pressure-shift-induced water adsorption in carbon micropores, Langmuir 17 (2001) 664–669.
[7] Y. Hanzawa, K. Kaneko, Lack of a predominant adsorption of water vapor on carbon mesopores, Langmuir 13 (1997) 5802–5804.
[8] T. Ohba, H. Kanoh, K. Kaneko, Affinity transformation from hydrophilicity to hydrophobicity of water molecules on the basis of adsorption of water in graphitic nanopores, J. Am. Chem. Soc. 126 (2004) 1560–1562.
[9] M. Thommes, J. Morell, K.A. Cychosz, M. Froba, Combining nitrogen, argon, and water adsorption for advanced characterization of ordered mesoporous carbons (CMKs) and periodic mesoporous organosilicas (PMOs), Langmuir 29 (2013) 14,893–14,902.
[10] A.V. Neimark, Y. Lin, P.I. Ravikovitch, M. Thommes, Quenched solid density functional theory and pore size analysis of micro-mesoporous carbons, Carbon 47 (2009) 1617–1628.
[11] K. Murata, K. Kaneko, W.A. Steele, F. Kokai, K. Takahashi, D. Kasuya, M. Yudasaka, S. Iijima, Porosity evaluation of intrinsic intraparticle nanopores of single wall carbon nanohorns, Nano Lett. 1 (2001) 197–199.
[12] M. Thommes, Physical adsorption characterization of nanoporous materials, Chem. Ing. Tech. 8 (2010) 1059–1073.
[13] P.J.F. Harris, Filled and heterogenous nanotubes, Carbon nanotube science, synthesis, properties and applications, Cambridge University Press, Cambridge 2009, pp. 247–274.
[14] T. Fujimori, K. Urita, D. Tománek, T. Ohba, I. Moriguchi, M. Endo, K. Kaneko, Selective probe of the morphology and local vibrations at carbon nanoasperities, J. Chem. Phys. 136 (2012) (064,505, 1–5).
[15] N.I. Kovtyukhova, T.E. Mallouk, L. Pan, E.C. Dickey, Individual single-walled nanotubes and hydrogels made by oxidative exfoliation of carbon nanotube ropes, J. Am. Chem. Soc. 125 (2003) 9761–9769.
[16] M.D. Ellison, P.J. Gasda, Functionalization of single-walled carbon nanotubes with 1,4-benzenediamine using a diazonium reaction, J. Phys. Chem. C 112 (2008) 738–740.
[17] R. Chand Bansal, J.-B. Donnet, F. Stoeckli, Active carbon, Marcel Dekker Inc., New York, 1988.
[18] E. Bekyarova, Y. Hanzawa, K. Kaneko, J. Silvestre-Albero, A. Sepulveda-Escribano, F. Rodriguez-Reinoso, D. Kasuya, M. Yudasaka, S. Iijima, Cluster-mediated filling of water vapor in intratube and interstitial nanospaces of single-wall carbon nanohorns, Chem. Phys. Lett. 366 (2002) 463–468.
[19] G.S. Szymanski, Z. Karpinski, S. Biniak, A. Swiatkowski, The effect of the gradual thermal decomposition of surface oxygen species on the chemical and catalytic properties of oxidized activated carbon, Carbon 40 (2002) 2627–2639.
[20] M. Nakamura, T. Ohba, P. Branton, H. Kanoh, K. Kaneko, Equilibration-time and pore-width dependent hysteresis of water adsorption isotherm on hydrophobic microporous carbons, Carbon 48 (2010) 305–312.